


# Experimental colitis in *IL-10*-deficient mice ameliorates in the absence of PTPN22

T. Jofra,<sup>\*1</sup> G. Galvani,<sup>\*1</sup>  
I. Cosorich,<sup>\*</sup> L. De Giorgi,<sup>\*</sup>  
A. Annoni,<sup>†</sup> A. Vecchione,<sup>\*</sup> C. Sorini,<sup>\*</sup>  
M. Falcone<sup>\*</sup> and G. Fousteri <sup>\*</sup>

<sup>\*</sup>Division of Immunology Transplantation and Infectious Diseases (DITID), Diabetes Research Institute (DRI), IRCCS San Raffaele Scientific Institute, and <sup>†</sup>San Raffaele Telethon Institute for Gene Therapy, IRCCS San Raffaele Scientific Institute, Milan, Italy

Accepted for publication 30 May 2019  
Correspondence: G. Fousteri, Division of Immunology Transplantation and Infectious Diseases (DITID), Diabetes Research Institute (DRI), IRCCS San Raffaele Scientific Institute, Milan, Italy.  
E-mail: fousteri.georgia@hsr.it

<sup>†</sup>These authors contributed equally to this study.

## Introduction

Inflammatory bowel diseases (IBD) are a group of heterogeneous diseases, and their main subforms are Crohn's disease (CD) and ulcerative colitis (UC). CD usually affects the distal ileum, but the diseases can be located anywhere from the oral cavity to the anus [1]. UC colitis is restricted to the colon and the inflammation is limited to the mucosa that affect the upper and lower gastrointestinal tract [2,3]. IBD is driven by aberrant activation of innate and adaptive immune responses. Genetic variants and alterations in the gut microflora strongly influence disease predisposition [2,3]. In IBD, genomewide association studies (GWAS) have identified single nucleotide polymorphisms (SNPs) in more than 160 risk genes [2,3]. Among the risk genes, those encoding for interleukin (IL)-10 and protein tyrosine phosphatase, non-receptor type 22

## Summary

Interleukin (IL)-10 plays a key role in controlling intestinal inflammation. *IL-10*-deficient mice and patients with mutations in *IL-10* or its receptor, *IL-10R*, show increased susceptibility to inflammatory bowel diseases (IBD). Protein tyrosine phosphatase, non-receptor type 22 (PTPN22) controls immune cell activation and the equilibrium between regulatory and effector T cells, playing an important role in controlling immune homeostasis of the gut. Here, we examined the role of PTPN22 in intestinal inflammation of *IL-10*-deficient (*IL-10*<sup>-/-</sup>) mice. We crossed *IL-10*<sup>-/-</sup> mice with *PTPN22*<sup>-/-</sup> mice to generate *PTPN22*<sup>-/-</sup>*IL-10*<sup>-/-</sup> double knock-out mice and induced colitis with dextran sodium sulphate (DSS). In line with previous reports, DSS-induced acute and chronic colitis was exacerbated in *IL-10*<sup>-/-</sup> mice compared to wild-type (WT) controls. However, *PTPN22*<sup>-/-</sup>*IL-10*<sup>-/-</sup> double knock-out mice developed milder disease compared to *IL-10*<sup>-/-</sup> mice. IL-17-promoting innate cytokines and T helper type 17 (Th17) cells were markedly increased in *PTPN22*<sup>-/-</sup>*IL-10*<sup>-/-</sup> mice, but did not provide a protective function. CXCL1/KC was also increased in *PTPN22*<sup>-/-</sup>*IL-10*<sup>-/-</sup> mice, but therapeutic injection of CXCL1/KC in *IL-10*<sup>-/-</sup> mice did not ameliorate colitis. These results show that PTPN22 promotes intestinal inflammation in *IL-10*-deficient mice, suggesting that therapeutic targeting of PTPN22 might be beneficial in patients with IBD and mutations in *IL-10* and *IL-10R*.

**Keywords:** colitis, IL-10, inflammatory bowel diseases (IBD), PTPN22

(PTPN22) have been strongly associated with enhanced and reduced risk to IBD, respectively [2,3].

The importance of IL-10 in intestinal homeostasis was shown in patients with early-onset IBD who carried pathogenic variants in *IL-10* and *IL-10R* [4]. IL-10 is a potent anti-inflammatory cytokine that inhibits T cell differentiation, proliferation and effector function, and exerts a protective role against IBD [5]. *IL-10*-deficient mice develop spontaneous IBD characterized by the presence of inflammatory infiltrates made up of lymphocytes, macrophages and neutrophils [6,7]. In line with this, inflammation develops in mice treated with neutralizing anti-IL-10R [8], confirming the essential role of IL-10 in intestinal homeostasis.

Genetic variants in *PTPN22*, and particularly the most well-known variant R620W (C1858T), were shown to be associated with a reduced risk for Crohn's disease in

humans [9,10]. *PTPN22* encodes a lymphoid tyrosine phosphatase that is expressed by both myeloid and lymphoid immune cells [3]. In T cells, *PTPN22* binds to C-terminal Src tyrosine kinase (Csk) and inhibits T cell receptor (TCR) signalling through dephosphorylation of the Lck protein tyrosine kinase [11,12]. Consequently, *PTPN22* impacts T cell signalling, activation and function [13]. *PTPN22*-deficient mice show lymphoproliferation and effector memory T cell accumulation, but do not progress to autoimmunity due to an expansion of forkhead box protein 3 (FoxP3)<sup>+</sup>, regulatory T (T<sub>reg</sub>) and type 1 regulatory (Tr1) cells [14,15].

The role of *PTPN22* in intestinal homeostasis has been extensively studied in two mouse models of experimental colitis. In a T cell-mediated model of experimental colitis, transfer of naive *PTPN22*-deficient CD4<sup>+</sup> T cells into immunodeficient mice induced aggravated intestinal inflammation compared to *PTPN22*-wild-type (WT) naive CD4<sup>+</sup> T cells [15]. Transfer of *PTPN22*-deficient but not *PTPN22*-sufficient T<sub>reg</sub>s protected from colitis in this setting due to an enhanced capacity of *PTPN22*-deficient T<sub>reg</sub>s in expressing lymphocyte function-associated antigen 1 (LFA-1) and producing IL-10, compared to WT T<sub>reg</sub>s [15–17]. A protective role for *PTPN22* was shown in studies of dextran sodium sulphate (DSS)-induced acute colitis [18–20]. In these studies, lack of *PTPN22* aggravated weight loss and exacerbated intestinal inflammation. The mechanism by which *PTPN22* deficiency exacerbated DSS-induced acute colitis is still unclear, and so far has been attributed to a reduced type I interferon production and an altered macrophage polarization [18,19]. The role of *PTPN22* in human IBD is unclear [3]. One study found that patients with IBD showed reduced levels of *PTPN22* in the intestine, and specifically in their myeloid cells. Given the dual role of *PTPN22* in restricting proinflammatory but also regulatory responses, we sought to investigate its biological significance in the IL-10-deficient background by assessing colitis susceptibility in double knock-out *PTPN22*<sup>-/-</sup>*IL-10*<sup>-/-</sup> mice.

## Materials and methods

### Mice

*PTPN22*<sup>-/-</sup> mice and *IL-10*<sup>-/-</sup> (C57BL/6 background) were bred in-house as previously described [21]. *PTPN22*<sup>-/-</sup>*IL-10*<sup>-/-</sup> double knock-out mice were obtained by crossing *PTPN22*<sup>-/-</sup> mice and *IL-10*<sup>-/-</sup> and intercrossing the F1, and by crossing F2 *PTPN22*<sup>+/-</sup>*IL-10*<sup>-/-</sup> mice with *PTPN22*<sup>+/-</sup>*IL-10*<sup>+/-</sup> or *PTPN22*<sup>+/-</sup>*IL-10*<sup>-/-</sup> mice. The genetic background of the mice was tested by polymerase chain reaction (PCR). All mice were housed under specific pathogen-free conditions at the San Raffaele Scientific Institute in

compliance with guidelines of the Institutional Animal Care and Use Committee (IACUC #677).

### DSS-induced acute and chronic colitis

Acute DSS-induced colitis was induced in female mice (average age 18.89 ± 7.75 weeks) by adding 2.5% (weight/volume) dextran sodium sulphate (DSS) (mol. wt 40 kD; TdB Consultancy, Uppsala, Sweden) to the drinking water [22]. Mice were first treated for 7 days with DSS and then stabilized with normal drinking water for the following 2 days. Mice were euthanized 9 days after DSS treatment. For chronic DSS-induced colitis, mice were treated with two cycles of DSS (2.5%) for 7 days/cycle and 14 days of normal drinking water in between. Mice were monitored daily before and after oral DSS conditioning. Body weight was assessed regularly (daily during the first 7 days) and mice were euthanized when they had lost more than 30% of their initial body weight. Mesenteric lymph nodes (MLN), spleen and large intestine (LI) were collected 9 days after the initial DSS treatment. Spleen weight and the LI length were also recorded.

### Monoclonal anti-mouse IL-17A and recombinant CXCL1/KC treatments

The neutralizing rat anti-mouse IL-17A monoclonal antibody (mAb) was purchased from BioXCell (clone: 17F3; Cat #: BE0173). At the start of the DSS exposure, 100 µg of anti-IL-17A was administered intraperitoneally (i.p.) and administration of the same dose of mAb was repeated every 48 h for the duration of the experiment. Mouse recombinant CXCL1/KC was purchased from Biolegend (Cat. no. 573702); 100 ng of CXCL1/KC [in phosphate-buffered saline (PBS)] was administered i.p. starting on the day of DSS treatment and injections continued daily for the whole duration of the experiment.

### Cell isolation

Single-cell suspensions of MLN were prepared by mechanical crushing with the end of a syringe plunger. Cells were subsequently passed through a 40-µm nylon mesh cell strainer (Falcon, SACCO S.R.L., Cadorago, Italy) to remove aggregates. Large intestine was excised and mononuclear cells were isolated according to the protocol for isolation of murine lamina propria mononuclear cells, as previously described [23]. Briefly, after removing the colonic patches, tissue was cleaned with PBS, opened longitudinally and then predigested twice in Hanks's balanced salt solution (HBSS) without Ca<sup>2+</sup> and Mg<sup>2+</sup> with [1 mM dithiothreitol (DTT), 5 mM ethylenediamine tetraacetic acid (EDTA)] for 20 min at 37°C in a shaking incubator. After removing the adipose tissue, the LI was cut into pieces 1–2 mm long and incubated in a digestion solution (HBSS containing 0.5 mg/ml collagenase D (Roche, Basel, Switzerland),

1 mg/ml Dispase II (Roche) and 5 U/ml DNase I (Sigma, St Louis, MO, USA). The isolated cells were washed, resuspended in 5 ml of 40% Percoll (Sigma) and overlaid on 2.5 ml of 80% Percoll in a 15-ml Falcon tube and centrifuged for 20 min at 1000 g. The interphase containing the mononuclear cells was collected, filtered and centrifuged for 10 min at 500 g. The resulting cells were then used for flow cytometry analysis.

### Flow cytometry

Following a 2.4G2 (Fc) blocking step, cell surface staining was performed with anti-mouse CD3, CD4, CD25, CD45, CD44, CD8, CD62L, LFA-1, Ly6C, I-Ab, CD11b, F4/80, Ly6G and CD11c mAbs at 1 : 100 dilution in staining buffer [PBS, 2% fetal calf serum (FCS), 0.1% NaN<sub>3</sub>] (a list of the mAbs is shown in Supporting information, Table S1). To detect FoxP3, cells were treated and stained with the FoxP3 fixation/permeabilization kit, according to the manufacturer's instructions (eBioscience, San Diego, CA, USA). For cytokine analysis, cells were resuspended at a concentration 5–10 × 10<sup>6</sup>/ml in 10% cRPMI and activated in 96-well plates, by plating 100 µl (0.5–1 × 10<sup>6</sup> cells). Cells were activated with the addition of 0.5 µl (in 100 µl) of leucocyte activation cocktail (LAC, BD Biosciences, San Jose, CA, USA) containing phorbol myristate acetate (PMA)/ionomycin for 3 h and stained as described above. All samples were acquired using fluorescence activated cell sorter (FACS) Canto flow cytometer (BD Biosciences) and analysed with FlowJo software (Tree Star, Ashland, OR, USA).

### Serum cytokines and chemokines

The concentration of cytokines/chemokines in the serum was measured 1 day before and 3 days post-DSS treatment using a mouse cytokine 23-plex (Bio-Plex Pro Mouse Cytokine 23-plex Assay, Cat. no. M60009RDPD), according to the manufacturer's instructions (Bio-Rad, Hercules, CA, USA) and analysed using Bio-Plex Manager software. The kit consisted of the following cytokines/chemokines: IL-1α, IL-1β, IL-2, IL-3, IL-4, IL-5, IL-6, IL-9, IL-10, IL-12 subunit p40 [IL-12(p40)], IL-12(p70), IL-13, IL-17, IL-18, eotaxin, granulocyte colony-stimulating factor (G-CSF), granulocyte-macrophage colony-stimulating factor (GM-CSF), interferon (IFN)-γ, keratinocyte chemoattractant (KC), monocyte chemoattractant protein (MCP)-1, macrophage inflammatory protein (MIP)-1α, macrophage inflammatory protein (MIP)-1β, regulated upon activation, normal T cell expressed, and secreted (RANTES) and tumour necrosis factor (TNF).

### Histopathological analysis

For post-mortem histopathology, murine colons were excised, fixed in zinc-formalin (Sigma) and embedded in paraffin. Serial 4-µm sections were stained with haematoxylin and eosin (H&E) and images were acquired using Aperio AT2

(Leica Biosystems, Wetzlar, Germany). For colitis score assessment, the entire digital images were analysed based on (i) enterocytes loss, (ii) crypt inflammation, (iii) infiltration of mononuclear cells and (iv) polymorphonuclear leucocytes in the lamina propria and (v) epithelial hyperplasia, as described previously by Kennedy *et al.* [24]. Final colitis scores were expressed in a range from 0 to 15 to describe healthy and severe conditions, respectively.

### Statistical analysis

Weight loss curves were compared with the two-way analysis of variance (ANOVA) test followed by Bonferroni's post-test to compare replicate means for each time-point. Comparisons between groups were performed using Kruskal–Wallis analysis followed by Dunn's post-test (one-way ANOVA test) or a Mann–Whitney *U*-test where appropriate. In all cases the Prism software (GraphPad, La Jolla, CA, USA) was used. All error bars indicate standard error of the mean (s.e.m.), while horizontal lines show the mean. Asterisks in the graphs indicate significant *P*-values as follows: \**P* < 0.05, \*\**P* < 0.01, \*\*\**P* < 0.001 and \*\*\*\**P* < 0.0001.

## Results

### PTPN22 promotes acute experimental colitis in IL-10-deficient mice

In order to address the effect of PTPN22 in the intestinal inflammation of IL-10-deficient, *PTPN22* and *IL-10* double knock-out (*PTPN22*<sup>-/-</sup>*IL-10*<sup>-/-</sup>) mice were generated. *IL-10*-deficient (*IL-10*<sup>-/-</sup>) and *PTPN22*<sup>-/-</sup>*IL-10*<sup>-/-</sup> double knock-out mice were monitored for up to 24 weeks of age and no significant signs of spontaneous colitis were observed macroscopically (no weight loss, reduction in gut length or presence of loose stools) (Supporting information, Fig. S1). WT, *IL-10*<sup>-/-</sup>, *PTPN22*<sup>-/-</sup> and *PTPN22*<sup>-/-</sup>*IL-10*<sup>-/-</sup> mice were treated with DSS to induce acute colitis and mouse body weight was evaluated daily. While *IL-10*<sup>-/-</sup> and *PTPN22*<sup>-/-</sup> mice showed aggravated body weight loss compared to WT mice, body weight loss in *PTPN22*<sup>-/-</sup>*IL-10*<sup>-/-</sup> mice was similar to that observed in WT mice (Fig. 1a,b, Table 1). Thus, *PTPN22*<sup>-/-</sup>*IL-10*<sup>-/-</sup> mice were less susceptible to acute DSS-induced acute colitis compared to *IL-10*<sup>-/-</sup> and *PTPN22*<sup>-/-</sup> mice. *PTPN22*<sup>-/-</sup> and *IL-10*<sup>-/-</sup> mice had shorter colons and a higher degree of gut inflammation compared to WT controls (Fig. 1c–e), confirming previous data concerning the protective role of *IL-10* and *PTPN22* in DSS-induced acute colitis in mice [18,19,25]. Instead, *PTPN22*<sup>-/-</sup>*IL-10*<sup>-/-</sup> mice had longer colons and showed reduced gut inflammation compared to single knock-out, *IL-10*<sup>-/-</sup> and *PTPN22*<sup>-/-</sup> mice (Fig. 1d,e). Also, DSS-treated *IL-10*<sup>-/-</sup> mice had smaller spleens compared to *PTPN22*<sup>-/-</sup>*IL-10*<sup>-/-</sup> mice (Fig. 1f). No significant differences in the spleen size were

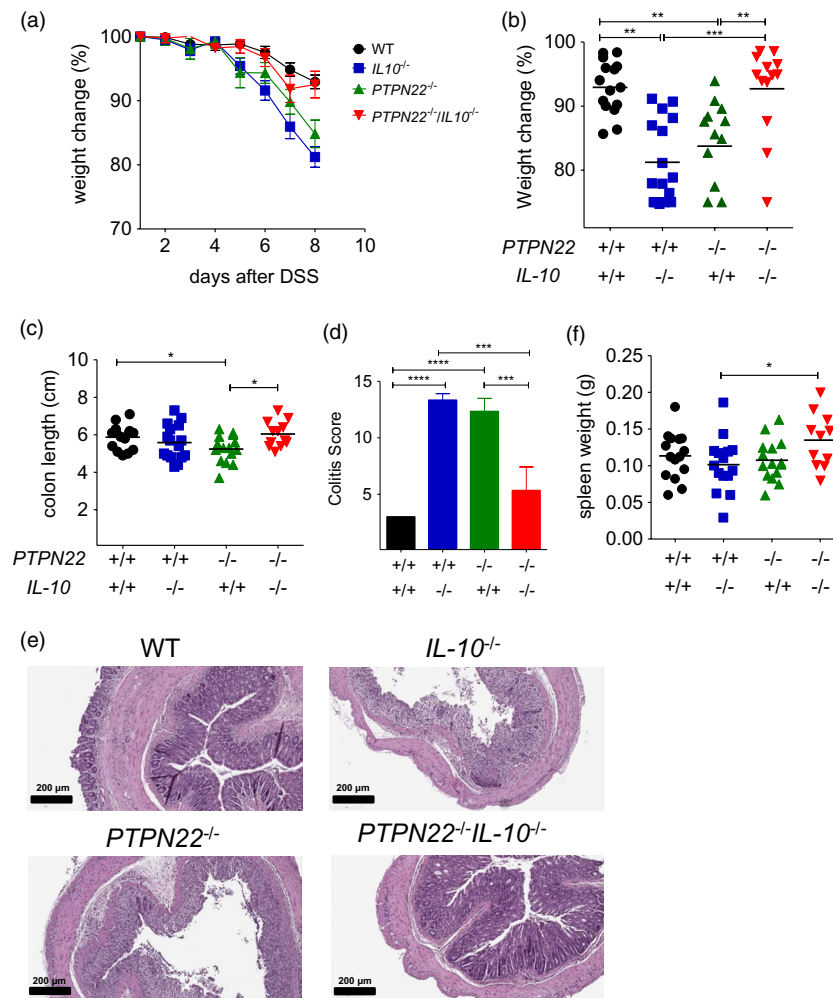


**Fig. 1.** Protein tyrosine phosphatase, non-receptor type 22 (PTPN22) promotes acute dextran sodium sulphate (DSS)-induced experimental colitis in *IL-10*-deficient mice. (a) Weight was measured in DSS-treated mice daily [wild-type (WT),  $n = 15$ ; *PTPN22*<sup>-/-</sup>,  $n = 15$ ; *IL-10*<sup>-/-</sup>,  $n = 17$  and *PTPN22*<sup>-/-</sup>*IL-10*<sup>-/-</sup>,  $n = 13$ ]. Graph shows daily weight change (in percentage) compared to the initial weight. (b) Percentage of weight change from initial weight of DSS-treated mice of (a) analysed at day 8. (c) Colon length among DSS-treated mice at day 8 expressed in cm. (d,e) Colitis score and representative haematoxylin and eosin (H&E) colon sections from DSS-treated mice of the indicated genotypes ( $n = 3$ /group). Scale bars: 200  $\mu$ m, high-power fields. (f) Spleen weight in grams analysed in DSS-treated mice at day 8. Horizontal lines in (b,c,f) show the mean. Each symbol represents an individual mouse. Data are pooled from three experiments with similar results. Statistical significance was determined by Kruskal–Wallis analysis followed by Dunn's post-test [one-way analysis of variance (ANOVA) test] (\* $P < 0.05$ , \*\* $P < 0.01$  and \*\*\* $P < 0.001$ ).

observed in the steady state among the four groups (Supporting information, Fig. S1c). Taken together, our data show that *PTPN22* and *IL-10* prevent acute DSS-induced colitis in mice. However, in the absence of *PTPN22*, *IL-10*-deficient mice are less susceptible to acute DSS-induced colitis. Thus, *PTPN22* promotes colitis in *IL-10*-deficient mice.

### PTPN22 promotes chronic experimental colitis in mice

Acute colitis induction with DSS relies on barrier defects, and the main disease mediators are cells of the innate immune system [26]. Given that *PTPN22* affects both innate and adaptive immune responses, we additionally assessed the role of *PTPN22* in a model of chronic colitis that is

**Table 1.** Statistical analysis of weight change in mice shown in Fig. 1

	WT	<i>IL-10</i> <sup>-/-</sup>	<i>PTPN22</i> <sup>-/-</sup>	<i>PTPN22</i> <sup>-/-</sup> <i>IL-10</i> <sup>-/-</sup>
WT		***	*	n.s.
<i>IL-10</i> <sup>-/-</sup>	***		n.s.	***
<i>PTPN22</i> <sup>-/-</sup>	*	n.s.		n.s.
<i>PTPN22</i> <sup>-/-</sup> <i>IL-10</i> <sup>-/-</sup>	n.s.	***	n.s.	

\* $P < 0.05$ ; \*\* $P < 0.01$  and \*\*\* $P < 0.001$ ; n.s. = not statistically significant. WT = wild-type; IL = interleukin; *PTPN22* = protein tyrosine phosphatase, non-receptor type 22.

thought to be predominantly mediated by T cells [26]. Here, mice were treated with two cycles of DSS for 7 days/

cycle alternating 14 days of normal drinking water in between. Unlike acute colitis, *PTPN22*<sup>-/-</sup> mice developed chronic disease that was less severe compared to WT controls (Fig. 2a). Instead, *IL-10*<sup>-/-</sup> mice showed severe weight loss and had to be euthanized. Interestingly, *PTPN22*<sup>-/-</sup>*IL-10*<sup>-/-</sup> mice showed weight lost that was similar to that observed in WT mice. The mortality rate was also significant in these mice, but was reduced compared to *IL-10*<sup>-/-</sup> mice (Fig. 2b). Taken together, these data suggest that lack of PTPN22 also protects mice from DSS-induced chronic colitis in the context of IL-10-deficiency (Table 2).

### PTPN22 and IL-10 control LFA-1 expression in FoxP3<sup>+</sup>CD4<sup>+</sup>T<sub>reg</sub> cells

In order to understand how *PTPN22* controls gut inflammation in an IL-10-sufficient and IL-10-deficient context, we analysed the frequency and phenotype of FoxP3<sup>+</sup>T<sub>reg</sub> cells, whose development and function is controlled by PTPN22 [15,16,27,28]. MLN and lymphocytes of the LI were collected 8 days after DSS treatment and stained for analysis. *PTPN22*<sup>-/-</sup> and *PTPN22*<sup>-/-</sup>*IL-10*<sup>-/-</sup> mice showed an increased percentage of FoxP3<sup>+</sup> and CD25<sup>+</sup>FoxP3<sup>+</sup> CD4<sup>+</sup>T cells (T<sub>reg</sub>) in their MLN compared to WT mice

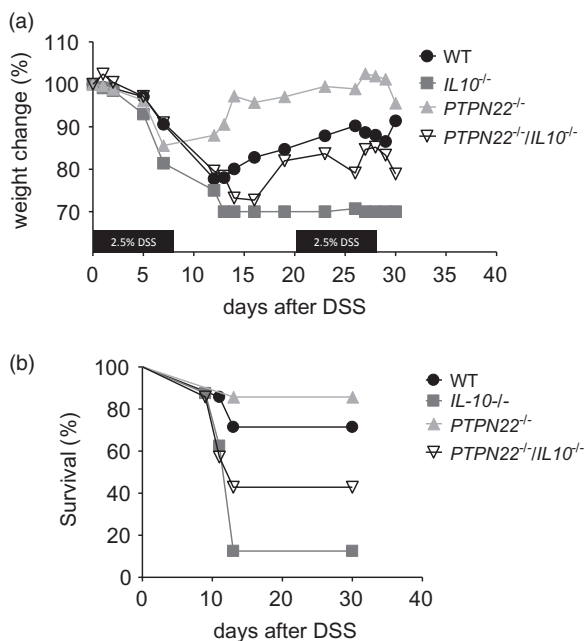


**Fig. 2.** Protein tyrosine phosphatase, non-receptor type 22 (PTPN22) promotes chronic dextran sodium sulphate (DSS)-induced experimental colitis. (a) Weight was measured in DSS-treated mice [wild-type (WT), *n* = 7; *PTPN22*<sup>-/-</sup>, *n* = 8; *IL-10*<sup>-/-</sup>, *n* = 7 and *PTPN22*<sup>-/-</sup>*IL-10*<sup>-/-</sup>, *n* = 7]. Graph shows weight change (in percentage) compared to the initial weight. The mice were followed until day 31. (b) Survival curve of mice exposed to DSS from days 1 to 31. The same mice as in (a) are included. Statistical analysis of weight change is summarized in Table 3.

**Table 2.** Statistical analysis of weight change in mice shown in Fig. 2

	WT	<i>IL-10</i> <sup>-/-</sup>	<i>PTPN22</i> <sup>-/-</sup>	<i>PTPN22</i> <sup>-/-</sup> <i>IL-10</i> <sup>-/-</sup>
WT		***	*	n.s.
<i>IL-10</i> <sup>-/-</sup>	***		*	*
<i>PTPN22</i> <sup>-/-</sup>	*	n.s.		n.s.
<i>PTPN22</i> <sup>-/-</sup> <i>IL-10</i> <sup>-/-</sup>	n.s.	*	*	

WT = wild-type; IL = interleukin; PTPN22 = protein tyrosine phosphatase, non-receptor type 22; n.s. = not significant.

**Table 3.** Summary of changes in T<sub>reg</sub> and Th17 subset distribution according to genotype in DSS-colitic mice

DSS colitic mice	mLN		LI	
	T <sub>reg</sub>	Th17	T <sub>reg</sub>	Th17
WT	=	=	=	=
<i>IL-10</i> <sup>-/-</sup>	=	=	=	↑
<i>PTPN22</i> <sup>-/-</sup>	↑	=	=	=
<i>PTPN22</i> <sup>-/-</sup> <i>IL-10</i> <sup>-/-</sup>	↑	↑	=	↑

WT = wild-type; IL = interleukin; PTPN22 = protein tyrosine phosphatase, non-receptor type 22; T<sub>reg</sub> = regulatory T cells; Th17 = T helper type 17; mLN = mesenteric lymph nodes; LI = large intestine; DSS = dextran sodium sulphate.

(Fig. 3a,b and Supporting information, Fig. S2 for gating strategy). Instead, *IL-10*<sup>-/-</sup> mice showed a reduction in T<sub>reg</sub> cells in the LI compared to WT and *PTPN22*<sup>-/-</sup> mice (Fig. 3c and Table 3). To address whether this effect was specific to the DSS-induced inflammation, we evaluated the frequency of T<sub>reg</sub> cells in the steady state. T<sub>reg</sub> cell frequency was found elevated in the MLN and LI of *PTPN22*<sup>-/-</sup> and *PTPN22*<sup>-/-</sup>*IL-10*<sup>-/-</sup> mice compared to WT controls (Supporting information, Fig. S3b,c), suggesting that PTPN22 controls T<sub>reg</sub> cell development in the MLN both in the steady state and under inflammatory conditions.

Recent results have shown that T<sub>reg</sub> cells need to express LFA-1 to mediate their suppressive function and that PTPN22 controls LFA-1 expression in T<sub>reg</sub> cells [17,29]. Here, we analysed the expression levels of LFA-1 on FoxP3<sup>+</sup>T<sub>reg</sub> cells in the MLN and LI of the four groups of mice 8 days after DSS treatment. We found that *IL-10*<sup>-/-</sup>, *PTPN22*<sup>-/-</sup> and *PTPN22*<sup>-/-</sup>*IL-10*<sup>-/-</sup> mice showed elevated expression of LFA-1 on FoxP3<sup>+</sup>T<sub>reg</sub> cells from MLN in comparison to WT mice, while no differences were seen in the LI (Fig. 3d-f). Thus, our findings support a role for PTPN22 and IL-10 in LFA-1 expression levels by T<sub>regs</sub> in the MLN of colitic mice.

### IL-17 production is increased in the MLN and LI of *PTPN22*<sup>-/-</sup>*IL-10*<sup>-/-</sup> mice with colitis

Experimental colitis is mediated by effector T cells that home in the gut when the gut epithelial barrier is breached by

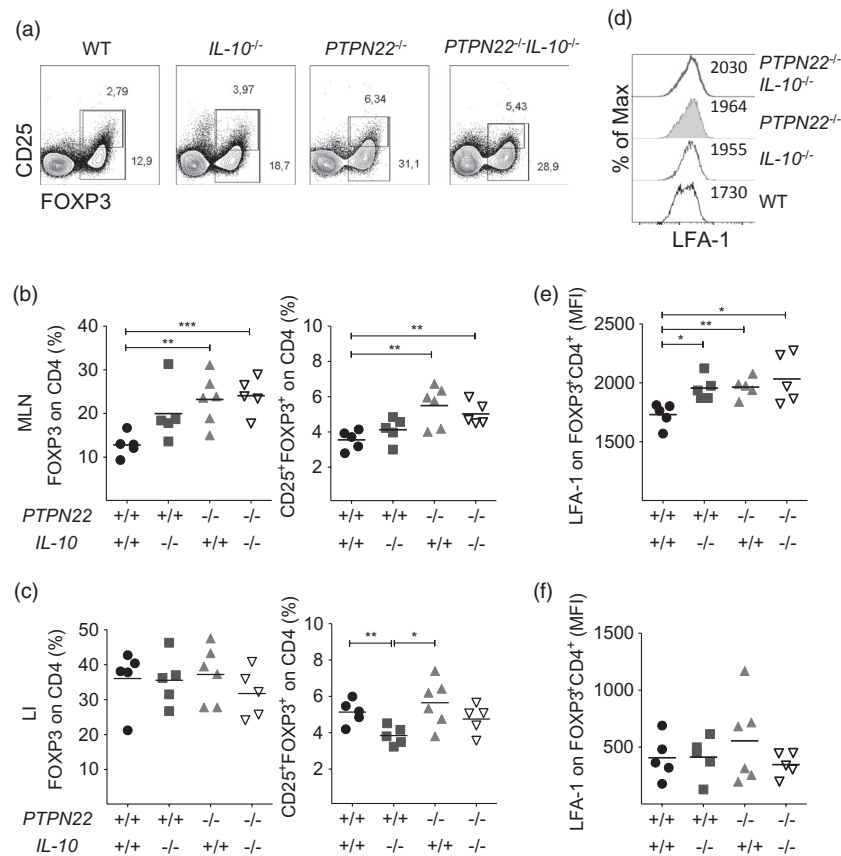


**Fig. 3.** Protein tyrosine phosphatase, non-receptor type 22 (PTPN22) controls the number of forkhead box protein 3 (FoxP3)<sup>+</sup> regulatory T cells (T<sub>reg</sub>) and their expression of lymphocyte function-associated antigen 1 (LFA-1) in colitic *IL-10*-deficient mice. (a) Representative fluorescence activated cell sorter (FACS) plots show frequency of FoxP3<sup>+</sup> and CD25<sup>+</sup>FoxP3<sup>+</sup> T<sub>reg</sub> cells in the mesenteric lymph nodes (MLN) of wild-type (WT), *PTPN22*<sup>-/-</sup>, *IL-10*<sup>-/-</sup> and *PTPN22*<sup>-/-</sup>*IL-10*<sup>-/-</sup> mice treated with dextran sodium sulphate (DSS) for 8 days. One representative mouse per group is shown. (b,c) Graphs display T<sub>reg</sub> frequencies in MLN (b) and large intestine (LI) (c) from multiple mice (*n* = 5–6/group). (d) Histogram overlay depicting LFA-1 expression levels (% of max.) on FoxP3<sup>+</sup> T<sub>reg</sub> cells from MLNs. (e,f) Mean fluorescence intensity (gMFI) of LFA-1 on FoxP3<sup>+</sup> T<sub>reg</sub> cells from MLN (e) and LI (f). Horizontal lines in (b,c) and (e,f) show mean. Each symbol represents an individual mouse. Data are pooled from two experiments with similar results. Statistical significance was determined by Kruskal–Wallis analysis followed by Dunn's post-test [one-way analysis of variance (ANOVA) test] (\**P* < 0.05, \*\**P* < 0.01 and \*\*\**P* < 0.001).

DSS and cause inflammation via the production of inflammatory cytokines, including IFN- $\gamma$ , TNF and IL-17 [30]. Here, we evaluated the profile of proinflammatory cytokine production by gut infiltrating lymphocytes. Co-staining for IFN- $\gamma$  and TNF identified three populations of CD4<sup>+</sup> T cells in the MLN and LI: IFN- $\gamma$ <sup>-</sup>TNF<sup>+</sup>, IFN- $\gamma$ <sup>+</sup>TNF<sup>+</sup> and IFN- $\gamma$ <sup>+</sup>TNF<sup>-</sup> cells (Supporting information, Fig. S4). No differences in the percentage of IFN- $\gamma$ <sup>+</sup>TNF<sup>+</sup> CD4<sup>+</sup> T cells were found in any of the groups (see Supporting information, Fig. S4 and S5 for gating strategy). Co-staining for IFN- $\gamma$  and IL-17 identified three subsets of CD4<sup>+</sup> T cells: IFN- $\gamma$ <sup>-</sup>IL-17<sup>+</sup> [T helper type 17 (Th17)], IFN- $\gamma$ <sup>+</sup>IL-17<sup>+</sup> (Th1/Th17) and IFN- $\gamma$ <sup>+</sup>IL-17<sup>-</sup> (Th1) (Fig. 4a). The proportion of Th17 cells was significantly elevated in the MLN and LI of *PTPN22*<sup>-/-</sup>*IL-10*<sup>-/-</sup> mice compared to the other groups (Fig. 4b,c, left panels and see Supporting information, Fig. S5 for gating strategy). Moreover, the proportion of

Th1/Th17 cells was also increased in the MLN and LI of the *PTPN22*<sup>-/-</sup>*IL-10*<sup>-/-</sup> mice compared to the other groups (Fig. 4b,c, middle panels). Instead, the proportion of Th1 cells was higher in the MLN of *PTPN22*<sup>-/-</sup>*IL-10*<sup>-/-</sup> and *PTPN22*<sup>-/-</sup> mice compared to WT controls (Fig. 4b,c, right panels). Taken together, IL-17 production by CD4<sup>+</sup> T cells was found significantly elevated in the MLN and LI of *PTPN22*<sup>-/-</sup>*IL-10*<sup>-/-</sup> mice compared to *PTPN22*<sup>-/-</sup>, *IL-10*<sup>-/-</sup> and WT mice (Table 3).

It has been previously reported that CD8<sup>+</sup> T cells also participate in the intestinal inflammatory process of the gut mucosa [31]. Hence, we also analysed the cytokine profile of gut infiltrating CD8<sup>+</sup> T cells. Similarly to CD4<sup>+</sup> T cells, cytokine-producing CD8<sup>+</sup> T cells were grouped into six subsets according to their cytokine expression profile (Fig. 5a and Supporting information, Fig. S6a). The percentage of IFN- $\gamma$ <sup>+</sup>TNF<sup>+</sup> CD8<sup>+</sup> T cells was increased in the MLN of *PTPN22*<sup>-/-</sup>*IL-10*<sup>-/-</sup> mice

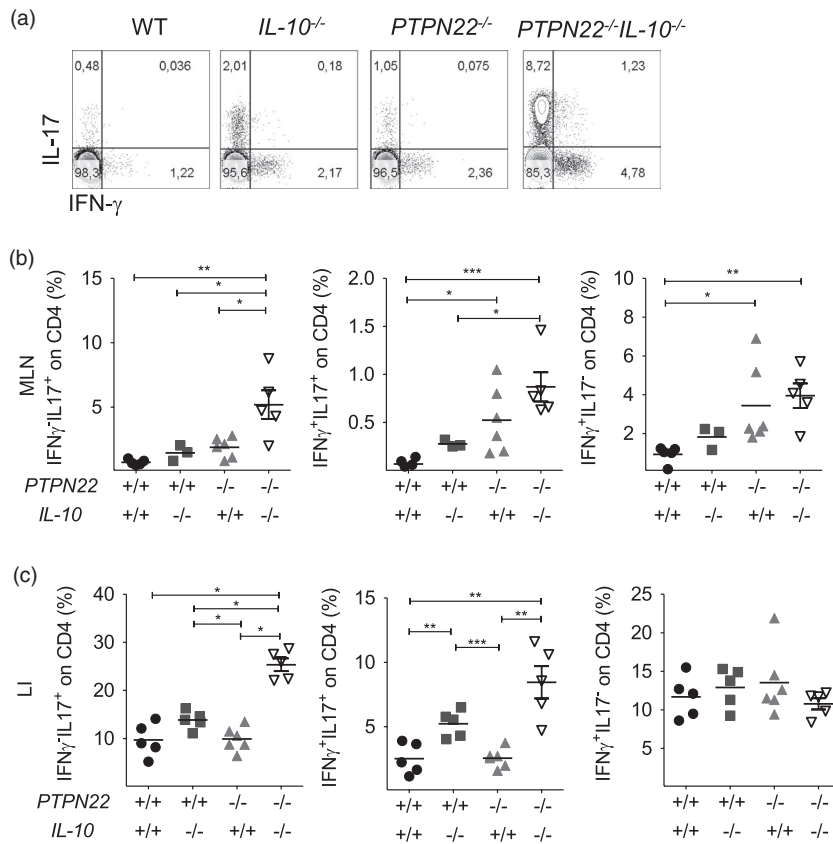


**Fig. 4.** Protein tyrosine phosphatase, non-receptor type 22 (PTPN22) restricts interleukin (IL)-17 production by CD4 T cells in *IL-10*-deficient mice treated with dextran sodium sulphate (DSS). Lamina propria mononuclear cells from WT, *PTPN22*<sup>-/-</sup>, *IL-10*<sup>-/-</sup> and *PTPN22*<sup>-/-</sup>*IL-10*<sup>-/-</sup> mice treated with DSS for 8 days were processed, fixed, permeabilized and stained to assess interferon (IFN)- $\gamma$  and IL-17 by CD4<sup>+</sup> T cells. (a) Representative fluorescence activated cell sorter (FACS) plots display frequency of IFN- $\gamma$ <sup>+</sup>IL-17<sup>+</sup>, IFN- $\gamma$ <sup>+</sup>IL-17<sup>-</sup> and IFN- $\gamma$ <sup>-</sup>IL-17<sup>+</sup> CD4 T cells from the mesenteric lymph nodes (MLN). A representative mouse from each strain is shown. (b,c) Graphs display frequency in MLN (b) and large intestine (LI) (c) from multiple mice ( $n = 3-5$ /group). Horizontal lines show mean. Each symbol represents an individual mouse. Data are pooled from two experiments with similar results. Statistical significance was determined by Kruskal-Wallis analysis followed by Dunn's post-test [one-way analysis of variance (ANOVA) test] (\* $P < 0.05$ , \*\* $P < 0.01$  and \*\*\* $P < 0.001$ ).

in comparison to *IL-10*<sup>-/-</sup> mice (Supporting information, Fig. S6a,b). While no significant differences in the percentage of IL-17 and IFN- $\gamma$ -expressing CD8<sup>+</sup> T cells were observed in MLN (Fig. 5b), analysis of LI showed a higher proportion of IL-17 and IFN- $\gamma$  co-expressing CD8<sup>+</sup> T cells of *PTPN22*<sup>-/-</sup>*IL-10*<sup>-/-</sup> mice in comparison to the other groups (Fig. 5c). Together, these data show that the proportion of IL-17-producing CD4<sup>+</sup> and CD8<sup>+</sup> T cells are increased in the gut of *PTPN22*<sup>-/-</sup>*IL-10*<sup>-/-</sup> mice compared to *PTPN22*<sup>-/-</sup>, *IL-10*<sup>-/-</sup> mice and WT controls.

#### PTPN22 controls DSS-induced innate proinflammatory cytokine production

Innate immune cells of myeloid origin and antigen-presenting cells (APC), e.g. dendritic cells (DCs), that infiltrate the inflamed lamina propria have been shown to sustain and propagate intestinal inflammation [32–35]. Here, we

analysed the frequency of F4/80<sup>+</sup> monocytes/macrophages and eosinophils, CD11b<sup>+</sup>Ly6G<sup>+</sup> neutrophils and CD11c<sup>+</sup> and CD11b<sup>+</sup>CD11c<sup>+</sup> DCs in the LI of DSS-treated mice and observed no significant differences between the four group of mice (Supporting information, Fig. S7 for gating strategy and Supporting information, Fig. S8 for data). Next, we assessed by Bio-Plex the serum levels of 23 cytokines and chemokines that could be involved in intestinal inflammation. Serum was collected 3 days after the initiation of DSS and eight cytokines/chemokines were found significantly elevated in *PTPN22*<sup>-/-</sup>*IL-10*<sup>-/-</sup> mice: IL-1b, IL-6, IL-12 (p40), IL-2, MIP-1a, MIP-1b, CXCL1/KC, MCP-1 and RANTES (Fig. 6).

#### Blockade of IL-17 does not worsen DSS-induced acute colitis in of *PTPN22*<sup>-/-</sup>*IL-10*<sup>-/-</sup> mice

IL-1b, IL-6 and IL-12 (p40) comprise part of the group of innate cytokines that promote Th17 polarization [36].

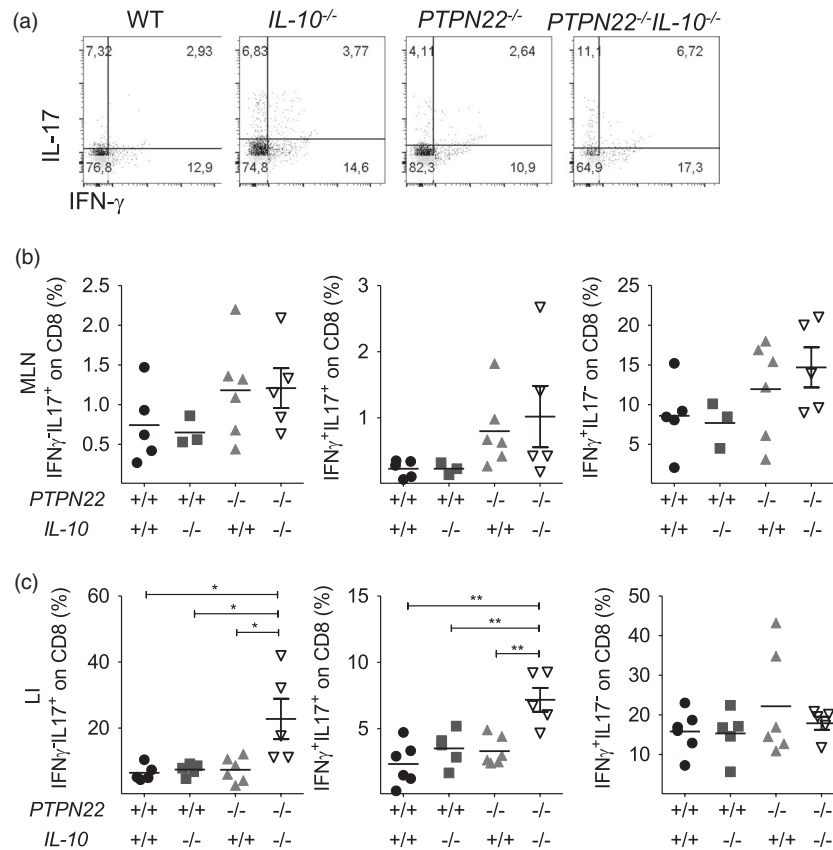


**Fig. 5.** Protein tyrosine phosphatase, non-receptor type 22 (*PTPN22*) restricts interleukin (IL)-17 production by CD8 T cells in *IL-10*-deficient mice treated with dextran sodium sulphate (DSS). Wild-type (WT), *PTPN22*<sup>-/-</sup>, *IL-10*<sup>-/-</sup> and *PTPN22*<sup>-/-</sup>*IL-10*<sup>-/-</sup> mice were treated with DSS for 8 days and their mesenteric lymph node (MLN) and large intestine (LI) were processed, fixed, permeabilized and stained to assess interferon (IFN)-γ and IL-17 by CD8<sup>+</sup> T cells. (a) Representative fluorescence activated cell sorter (FACS) plots display frequency of IFN-γ<sup>+</sup>IL-17<sup>+</sup>, IFN-γ<sup>+</sup>IL-17<sup>+</sup> and IFN-γ<sup>+</sup>IL-17<sup>+</sup> CD8 T cells from the LI. A representative mouse from each strain is shown. (b,c) Graphs display frequency in MLN (b) and LI (c) from multiple mice (*n* = 5/group). Horizontal lines show mean. Each symbol represents an individual mouse. Data are pooled from two experiments with similar results. Statistical significance was determined by Kruskal–Wallis analysis followed by Dunn’s post-test [one-way analysis of variance (ANOVA) test] (\**P* < 0.05, \*\**P* < 0.01 and \*\*\**P* < 0.001).

The increased levels of these cytokine mediators in the sera of *PTPN22*<sup>-/-</sup>*IL-10*<sup>-/-</sup> mice (Fig. 6) are in line with the elevated levels of Th17 cells found in their gut (Fig. 4c). Two recent independent reports by Ogawa *et al.* [37] and O’Connor *et al.* [38] showed that IL-17 can exert a protective role from colitis and maintain gut homeostasis by suppressing Th1 differentiation. Therefore, we hypothesized that the production of IL-17-promoting cytokines and T cell-derived IL-17 might be the reason for disease protection in *PTPN22*<sup>-/-</sup>*IL-10*<sup>-/-</sup> mice. Consequently, *PTPN22*<sup>-/-</sup>*IL-10*<sup>-/-</sup> mice were treated with anti-IL-17A and monitored for weight loss. In contrast to our initial hypothesis, IL-17A blockade did not worsen acute DSS-induced colitis in *PTPN22*<sup>-/-</sup>*IL-10*<sup>-/-</sup> mice (Fig. 7a). Colon length was found increased in *PTPN22*<sup>-/-</sup>*IL-10*<sup>-/-</sup> mice treated with anti-IL-17A, suggesting that IL-17 played a proinflammatory rather

than a protective role (Fig. 7b). These findings suggest that neither IL-17 nor IL-17-promoting innate cytokines mediated protection from colitis *PTPN22*<sup>-/-</sup>*IL-10*<sup>-/-</sup> mice [39,40].

#### CXCL1/KC administration delays but does not protect from acute colitis *IL-10*-deficient mice

Given the elevated levels of CXCL1/KC in the sera *IL-10*<sup>-/-</sup> mice, we thought to determine the role of CXCL1/KC in their intestinal response to inflammation. Earlier studies by Donohue *et al.* showed that mice with a targeted mutation in CXCL1/KC exhibit a much more profound colitis in response to DSS, supporting a protective role of CXCL1/KC in this disease [41]. Consequently, we hypothesized that the increased levels of CXCL1/KC in the sera of *PTPN22*<sup>-/-</sup>*IL-10*<sup>-/-</sup> mice might have had an anti-inflammatory activity. To test this hypothesis, we



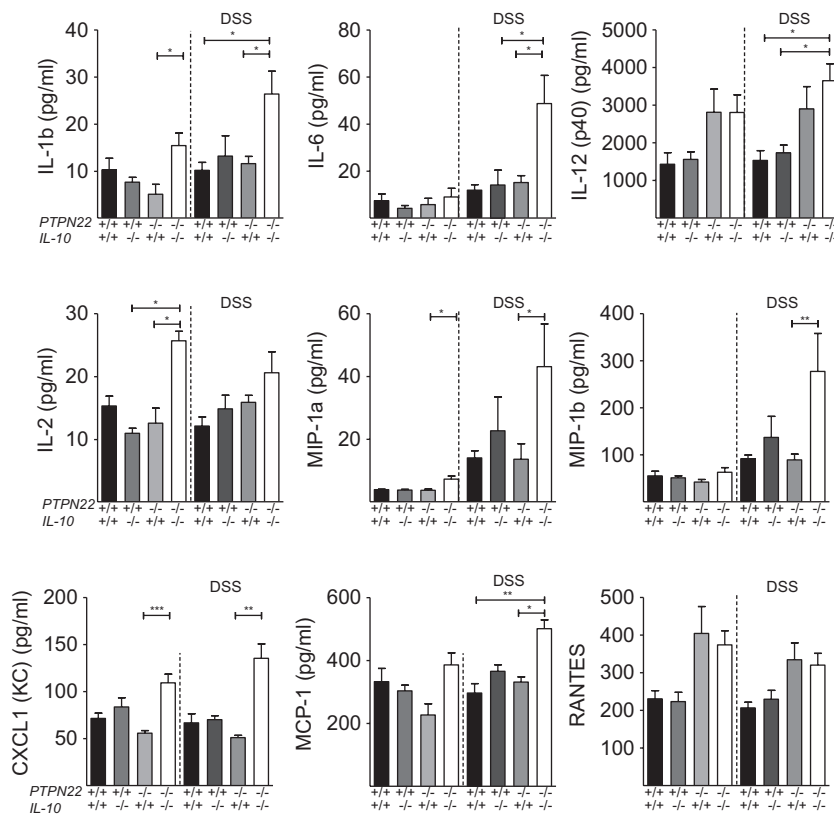


**Fig. 6.** Innate serum cytokine and chemokine analysis with Bio-Plex. Serum was collected on day 3 after dextran sodium sulphate (DSS) treatment. (a) Plots show levels of between interleukin (IL)-1b, IL-6, IL-12 (p40), IL-2, macrophage inflammatory protein (MIP)-1 $\alpha$ , MIP-1 $\beta$ , chemokine (C-X-C motif) ligand 1 (CXCL1) (KC), monocyte chemoattractant protein (MCP)-1 and regulated upon activation, normal T cell expressed, and secreted (RANTES) in WT ( $n = 5$ ), protein tyrosine phosphatase, non-receptor type 22 ( $PTPN22^{-/-}$ ) ( $n = 5$ ),  $IL-10^{-/-}$  ( $n = 7$ ) and  $PTPN22^{-/-}IL-10^{-/-}$  ( $n = 7$ ) mice. Statistical significance was determined by Kruskal–Wallis analysis followed by Dunn’s post-test [one-way analysis of variance (ANOVA) test] ( $*P < 0.05$ ,  $**P < 0.01$  and  $***P < 0.001$ ). Each symbol represents an individual mouse.

administered recombinant CXCL1/KC to  $IL-10$ -deficient mice. We found that CXCL1/KC treatment delayed disease progression by a couple of days and, with the exception of one mouse that was protected from colitis, the remaining four CXCL1-treated mice developed wasting disease and acute colitis (Fig. 7c).

## Discussion

This study shows that  $PTPN22^{-/-}IL-10^{-/-}$  mice are less susceptible to acute DSS-induced experimental colitis compared to  $PTPN22^{-/-}$  and  $IL-10^{-/-}$  mice. This finding was surprising and unexpected, as both  $PTPN22^{-/-}$  and  $IL-10^{-/-}$  mice are more susceptible to acute DSS-colitis when compared to WT controls. Of note, neither  $IL-10^{-/-}$  nor  $PTPN22^{-/-}IL-10^{-/-}$  double knock-out mice showed any macroscopic evidence of autoimmunity or colitis in the steady state. We also found that PTPN22 is a promoter of chronic DSS-induced colitis in mice. Lack of PTPN22 protected from chronic DSS-induced colitis in both

$IL-10$ -sufficient and  $IL-10$ -deficient mice. These findings suggest a dual, context-dependent role of PTPN22: PTPN22 acts as a repressor of acute inflammatory immune responses in the gut in the presence of  $IL-10$ , but acts as a promoter of acute gut inflammation in the absence of  $IL-10$ . During chronic inflammation, however, PTPN22 promotes gut inflammation irrespective of the presence of  $IL-10$ .

Similarly to  $PTPN22^{-/-}$  mice,  $PTPN22^{-/-}IL-10^{-/-}$  mice had a substantial increase of MLN-residing  $T_{reg}$  cells ( $CD4^{+}FoxP3^{+}$ ) that expressed elevated levels LFA-1 compared to WT mice [17]. However, the elevation in  $FoxP3^{+}T_{reg}$  and LFA-1 levels probably played a minor role in protecting from acute DSS-colitis, as  $PTPN22^{-/-}$  mice were more susceptible to this form of colitis that is driven by an innate proinflammatory response [18,19]. However,  $T_{regs}$  might have played a role in protecting PTPN22-deficient from chronic colitis that is thought to be T cell-mediated.

Unfortunately, the use of littermates was not possible in all experiments. Consequently, microbiota could have

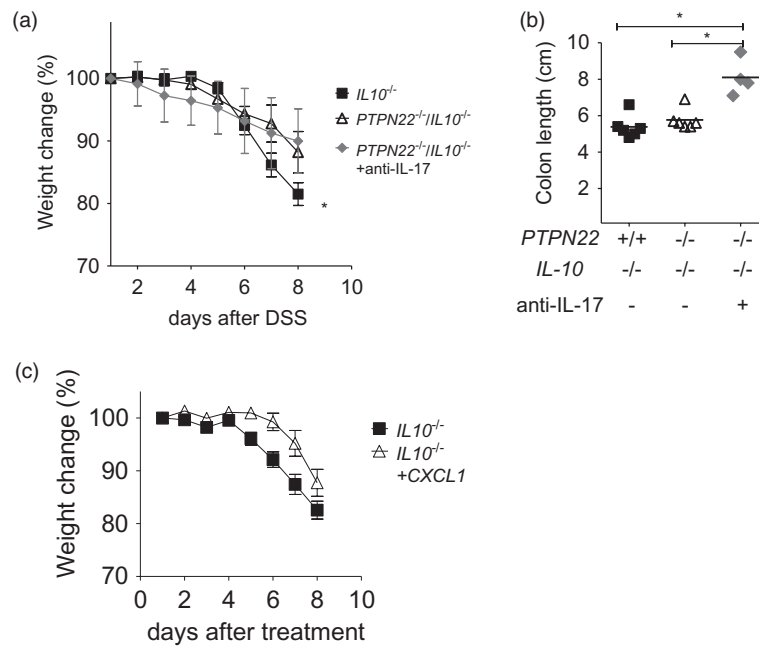


**Fig. 7.** Interleukin (IL)-17 blockade in protein tyrosine phosphatase, non-receptor type 22 (*PTPN22*<sup>-/-</sup>)*IL-10*<sup>-/-</sup> mice does not increase susceptibility to dextran sodium sulphate (DSS)-induced acute colitis. (a) Weight was measured in DSS-treated mice daily (*IL-10*<sup>-/-</sup>, *n* = 6, *PTPN22*<sup>-/-</sup>*IL-10*<sup>-/-</sup> *n* = 6 and *PTPN22*<sup>-/-</sup>*IL-10*<sup>-/-</sup> + anti-IL-17, *n* = 4). Graph shows daily weight change (in percentage) compared to the initial weight. (b) Colon length among DSS-treated mice at day 8 expressed in cm. (c) Weight was measured in DSS-treated mice daily (*IL-10*<sup>-/-</sup>, *n* = 18, *IL-10*<sup>-/-</sup> + CXCL1/KC, *n* = 5). Graph shows daily weight change (in percentage) between *IL-10*<sup>-/-</sup> and *IL-10*<sup>-/-</sup> mice, treated with CXCL1/KC, compared to the initial weight.

played a role in disease protection. To evaluate their contribution, we repeated some of the experiments by randomly mixing the mice and allowing them to exchange bedding material for 2 weeks prior to DSS treatment. The results obtained were similar (although repeated only twice; data not shown), suggesting that *PTPN22* promotes acute and chronic colitis in *IL-10*-deficient mice. Of note, in the chronic colitis experiments mice were treated with only two cycles of DSS. The experiment had to be interrupted because *IL-10*<sup>-/-</sup> mice showed severe weight loss (loss of 30% of initial body weight is considered as death) compared to the other strains and had to be euthanized.

The role of IL-10 in intestinal inflammation is well established, while that of the *PTPN22* is less understood [3]. Depending on the experimental system, and the cellular and molecular mechanisms that are involved, *PTPN22* R620W seems to act as a loss-of-function or gain-of-function variant [42–45]. Our data suggest that *PTPN22* promotes inflammation when the expression of IL-10 is perturbed. Hence, we hypothesize that if *PTPN22* R620W acts as a loss-of-function variant in IBD, then individuals with variants in both *IL-10* and *PTPN22* might be less susceptible to developing the disease. Inevitably, our work has some limitations, but it would be interesting to analyse the association between *IL-10/IL-10R* and *PTPN22* variants and susceptibility to IBD.

To address the mechanism by which *PTPN22* promotes gut inflammation in *IL-10*<sup>-/-</sup> mice, we analysed the innate and adaptive proinflammatory cytokine profile. IL-17-promoting innate cytokines and Th17 polarization were highly increased in *PTPN22*<sup>-/-</sup>*IL-10*<sup>-/-</sup> mice compared to the other strains. However, IL-17 blockade did not aggravate disease in *PTPN22*<sup>-/-</sup>*IL-10*<sup>-/-</sup> double knock-out mice, suggesting that the elevated levels of IL-17 were not involved in protection from DSS-induced colitis.

IBDs are the result of complex interactions between various signalling pathways and different cell types that interact through chemokines and cytokines in the intestine and in other parts of the lymphoid and non-lymphoid organs [46]. To clarify the regulatory pathway that was activated in *PTPN22*<sup>-/-</sup>*IL-10*<sup>-/-</sup> double knock-out mice and protected from colitis development, we decided to investigate the role of CXCL1/KC, a chemokine that is known to play a protective role from DSS-induced colitis in C57BL/6 mice [41]. We found that CXCL1/KC treatment delayed disease progression but did not protect *IL-10*<sup>-/-</sup> mice from acute colitis.

In summary, we have shown that *PTPN22* promotes gut inflammation in *IL-10*<sup>-/-</sup> colitic mice. Moreover, *PTPN22* restricts FoxP3 expression in CD4<sup>+</sup> T cells even in the absence of IL-10, and both molecules (*PTPN22* and IL-10) restrict LFA-1 expression in T<sub>reg</sub> cells. *PTPN22*

and IL-10 also restrict Th17 cells at the inflammatory site, but this mechanism is not responsible for preventing gut inflammation in *PTPN22<sup>-/-</sup>IL-10<sup>-/-</sup>* mice. Probably the prevention of excessive inflammatory response in *PTPN22<sup>-/-</sup>IL-10<sup>-/-</sup>* mice is determined by a combination of factors rather than an individual cytokine/chemokine. Although further studies are needed, our data provide new insights into the mechanism by which PTPN22 and IL-10 cooperate in defining innate immune responses, T<sub>reg</sub> and Th17 differentiation and influence the course of inflammatory conditions such as IBD.

## Acknowledgements

This study was supported by a Marie Curie Reintegration Grant to G. F. T. J.; G. G. performed experiments, analysed data and assisted with writing the manuscript. I. C., L. D. G. and C. S. assisted with the isolation of lamina propria mononuclear cells. A. A. performed Bio-Plex analyses. A. V. assisted with colitis scoring. M. F. reviewed the manuscript. G. F. oversaw the study, analysed data and wrote the manuscript.

## Disclosures

The authors have declared that no conflicts of interest exist.

## References

- Huang BL, Chandra S, Shih DQ. Skin manifestations of inflammatory bowel disease. *Front Physiol* 2012; **3**:13.
- Lees CW, Barrett JC, Parkes M, Satsangi J. New IBD genetics: common pathways with other diseases. *Gut* 2011; **60**:1739–53.
- Spalinger MR, Scharl M. The role for protein tyrosine phosphatase non-receptor type 22 in regulating intestinal homeostasis. *United Eur Gastroenterol J* 2016; **4**:325–32.
- Moran CJ, Walters TD, Guo CH *et al.* IL-10R polymorphisms are associated with very-early-onset ulcerative colitis. *Inflamm Bowel Dis* 2013; **19**:115–23.
- Kole A, Maloy KJ. Control of intestinal inflammation by interleukin-10. *Curr Top Microbiol Immunol* 2014; **380**:19–38.
- Keubler LM, Buettner M, Häger C, Bleich A. A multihit model: colitis lessons from the interleukin-10-deficient mouse. *Inflamm Bowel Dis* 2015; **21**:1967–75.
- Kiesler P, Fuss IJ, Strober W. Experimental models of inflammatory bowel diseases. *Cell Mol Gastroenterol Hepatol* 2015; **1**:154–70.
- Asseman C, Mauze S, Leach MW, Coffman RL, Powrie F. An essential role for interleukin 10 in the function of regulatory T cells that inhibit intestinal inflammation. *J Exp Med* 1999; **190**:995–1004.
- Diaz-Gallo LM, Espino-Paisán L, Fransen K *et al.* Differential association of two PTPN22 coding variants with Crohn's disease and ulcerative colitis. *Inflamm Bowel Dis* 2011; **17**:2287–94.
- Zheng J, Ibrahim S, Petersen F, Yu X. Meta-analysis reveals an association of PTPN22 C1858T with autoimmune diseases, which depends on the localization of the affected tissue. *Genes Immun* 2012; **13**:641–52.
- Davidson D, Veillette A. PTP-PEST, a scaffold protein tyrosine phosphatase, negatively regulates lymphocyte activation by targeting a unique set of substrates. *EMBO J* 2011; **20**:3414–26.
- Cloutier JF, Veillette A. Cooperative inhibition of T-cell antigen receptor signaling by a complex between a kinase and a phosphatase. *J Exp Med* 1999; **189**:111–21.
- Cloutier JF, Veillette A. Association of inhibitory tyrosine protein kinase p50csk with protein tyrosine phosphatase PEP in T cells and other hemopoietic cells. *EMBO J* 1996; **15**:4909–18.
- Hasegawa K, Martin F, Huang G, Tumas D, Diehl L, Chan CA. PEST domain-enriched tyrosine phosphatase (PEP) regulation of effector/memory T cells. *Science* 2004; **303**:685–9.
- Brownlie RJ, Miosge LA, Vassilakos D, Svensson LM, Cope A, Zamoyska R. Lack of the phosphatase PTPN22 increases adhesion of murine regulatory T cells to improve their immunosuppressive function. *Sci Signal* 2012; **5**:ra87.
- Maine CJ, Hamilton-Williams EE, Cheung J *et al.* PTPN22 alters the development of regulatory T cells in the thymus. *J Immunol* 2012; **188**:5267–75.
- Brownlie RJ, Miosge LA, Vassilakos D, Svensson LM, Cope A, Zamoyska R. Lack of PTPN22 increases LFA-1-dependent adhesion of murine regulatory T Cells improving their regulatory function. *Sci Signal* 2012; **5**:ra87.
- Wang Y, Shaked I, Stanford SM *et al.* The autoimmunity-associated gene PTPN22 potentiates Toll-like receptor-driven, type 1 interferon-dependent immunity. *Immunity* 2013; **39**:111–22.
- Chang HH, Miaw SC, Tseng W *et al.* PTPN22 modulates macrophage polarization and susceptibility to dextran sulfate sodium-induced colitis. *J Immunol* 2013; **191**:2134–43.
- Spalinger MR, Kasper S, Gottier C *et al.* NLRP3 tyrosine phosphorylation is controlled by protein tyrosine phosphatase PTPN22. *J Clin Invest* 2016; **126**:1783–800.
- Fousteri G, Jofra T, Debernardis I *et al.* The protein tyrosine phosphatase PTPN22 controls forkhead box protein 3 T regulatory cell induction but is dispensable for T helper type 1 cell polarization. *Clin Exp Immunol* 2014; **178**:178–89.
- Wirtz S, Neufert C, Weigmann B, Neurath MF. Chemically induced mouse models of intestinal inflammation. *Nat Protocols* 2007; **2**:541–6.
- Weigmann B, Tubbe I, Seidel D, Nicolaev A, Becker C, Neurath MF. Isolation and subsequent analysis of murine lamina propria mononuclear cells from colonic tissue. *Nat Protoc* 2007; **2**:2307–11.
- Kennedy RJ, Hoper M, Deodhar K, Erwin PJ, Kirk SJ, Gardiner KR. Interleukin 10-deficient colitis: new similarities to human inflammatory bowel disease. *Br J Surg* 2000; **87**:1346–51.

- 25 Keubler LM, Buettner M, Häger C, Bleich A. A multihit model: colitis lessons from the interleukin-10-deficient mouse. *Inflamm Bowel Dis* 2015; **21**:1967–75.
- 26 Chassaing B, Aitken JD, Malleshappa M, Vijay-Kumar M. Dextran sulfate sodium (DSS)-induced colitis in mice. *Curr Protoc Immunol* 2014; **104**:25.
- 27 Fousteri G, Liossis SNC, Battaglia M. Roles of the protein tyrosine phosphatase PTPN22 in immunity and autoimmunity. *Clin Immunol* 2013; **149**:556–65.
- 28 Zheng P, Kissler S. PTPN22 silencing in the NOD model indicates the type 1 diabetes-associated allele is not a loss-of-function variant. *Diabetes* 2013; **62**:896–904.
- 29 Wohler J, Bullard D, Schoeb T, Barnum S. LFA-1 is critical for regulatory T cell homeostasis and function. *Mol Immunol* 2009; **46**:2424–8.
- 30 Kiesler P, Fuss IJ, Strober W. Experimental models of inflammatory bowel diseases. *Cell Mol Gastroenterol Hepatol* 2015; **1**:154–70.
- 31 Nancey S, Holvöet S, Graber I *et al.* CD8<sup>+</sup> cytotoxic T cells induce relapsing colitis in normal mice. *Gastroenterology* 2006; **131**:485–96.
- 32 Vermeren S, Miles K, Chu JY, Salter D, Zamoyska R, Gray M. PTPN22 is a critical regulator of Fc $\gamma$  receptor-mediated neutrophil activation. *J Immunol* 2016; **197**:4771–4779.
- 33 Wéra O, Lancellotti P, Oury C. The dual role of neutrophils in inflammatory bowel diseases. *J Clin Med* 2016; **5**:118.
- 34 Cruickshank SM, English NR, Felsburg PJ, Carding SR. Characterization of colonic dendritic cells in normal and colitic mice. *World J Gastroenterol* 2005; **11**:6338–47.
- 35 Qualls JE, Tuna H, Kaplan AM, Cohen DA. Suppression of experimental colitis in mice by CD11c<sup>+</sup> dendritic cells. *Inflamm Bowel Dis* 2009; **15**:236–47.
- 36 Strober W, Fuss IJ. Pro-inflammatory cytokines in the pathogenesis of IBD. *Gastroenterology* 2011; **140**:1756–67.
- 37 Ogawa A, Andoh A, Araki Y, Bamba T, Fujiyama Y. Neutralization of interleukin-17 aggravates dextran sulfate sodium-induced colitis in mice. *Clin Immunol* 2004; **110**:55–62.
- 38 O'Connor W Jr, Kamanaka M, Booth CJ *et al.* A protective function for interleukin 17A in T cell-mediated intestinal inflammation. *Nat Immunol* 2009; **10**:603–9.
- 39 Feng T, Qin H, Wang L, Benveniste EN, Elson CO, Cong Y. Th17 cells induce colitis and promote Th1 cell responses through IL-17 induction of innate IL-12 and IL-23 production. *J Immunol* 2011; **186**:6313–8.
- 40 Ito R, Kita M, Shin-Ya M *et al.* Involvement of IL-17A in the pathogenesis of DSS-induced colitis in mice. *Biochem Biophys Res Comm* 2008; **377**:12–6.
- 41 Shea-Donohue T, Thomas K, Cody MJ *et al.* Mice deficient in the CXCR4 ligand, CXCL1 (KC/GRO- $\alpha$ ), exhibit increased susceptibility to dextran sodium sulfate (DSS)-induced colitis. *Innate Immun* 2008; **14**:117–24.
- 42 Zheng J, Petersen F, Yu X. The role of PTPN22 in autoimmunity: learning from mice. *Autoimmun Rev* 2014; **13**:266–71.
- 43 Zhang J, Zahir N, Jiang Q *et al.* The autoimmune disease-associated PTPN22 variant promotes calpain-mediated Lyp/Pep degradation associated with lymphocyte and dendritic cell hyperresponsiveness. *Nat Genet* 2011; **43**:902–7.
- 44 Vang T, Congia M, Macis MD *et al.* Autoimmune-associated lymphoid tyrosine phosphatase is a gain-of-function variant. *Nat Genet* 2005; **37**:1317–9.
- 45 Galvani G, Fousteri G. PTPN22 and islet-specific autoimmunity: what have the mouse models taught us? *World J Diabetes* 2017; **8**:330–6.
- 46 Singh UP, Singh NP, Murphy EA *et al.* Chemokine and cytokine levels in inflammatory bowel disease patients. *Cytokine* 2016; **77**:44–9.

## Supporting Information

Additional supporting information may be found in the online version of this article at the publisher's web site:

**Fig. S1.** (a) Weight was measured WT ( $n = 16$ ), *PTPN22*<sup>-/-</sup> ( $n = 12$ ), *IL-10*<sup>-/-</sup> ( $n = 17$ ) and *PTPN22*<sup>-/-</sup>*IL-10*<sup>-/-</sup> ( $n = 17$ ) mice at the steady-state. (b-c) Colon length and spleen weight were determined for the same group of mice ( $n = 6$ -9/group). Each symbol represents an individual mouse. Data are pooled from >3 experiments with similar results.

**Fig. S2.** Representative FACS plots showing gating strategy used to characterize FOXP3<sup>+</sup> and CD25<sup>+</sup>FOXP3<sup>+</sup> CD4 T cells. The representative sample is from LI.

**Fig. S3.** (a) Representative FACS plots show frequency of FOXP3<sup>+</sup> and CD25<sup>+</sup>FOXP3<sup>+</sup> Treg cells in the MLN of WT, *PTPN22*<sup>-/-</sup>, *IL-10*<sup>-/-</sup> and *PTPN22*<sup>-/-</sup>*IL-10*<sup>-/-</sup> mice at the steady state. One representative mouse per group is shown. (b-c) Graphs display Treg frequency in MLN (b) and LI (c) from multiple mice ( $n = 6$ -9/group). (d) Lamina propria mononuclear cells were stained to assess IFN- $\gamma$  and IL-17 by CD4<sup>+</sup> T cells. Results are from multiple mice ( $n = 3$ /group). Horizontal lines show mean. Each symbol represents an individual mouse. Statistical significance was determined by Kruskal-Wallis analysis followed by Dunn's post-test (1-way ANOVA test) (\* $P < 0.05$ ; \*\* $P < 0.01$  and \*\*\* $P < 0.001$ ).

**Fig. S4.** MLN and lamina propria mononuclear cells from WT, *PTPN22*<sup>-/-</sup>, *IL-10*<sup>-/-</sup>, and *PTPN22*<sup>-/-</sup>*IL-10*<sup>-/-</sup> mice treated with DSS for 8 days were processed, stained, fixed and permeabilized to assess IFN- $\gamma$  and TNF by CD4<sup>+</sup> T cells (a) Representative FACS plots display frequency of IFN- $\gamma$ <sup>+</sup>TNF<sup>+</sup>, IFN- $\gamma$ <sup>+</sup>TNF<sup>-</sup> and IFN- $\gamma$ <sup>-</sup>TNF<sup>+</sup> CD4 T cells from the LI. A representative mouse from each strain is shown. (b-c) Graphs display frequency in MLN (b) and LI (c) from multiple mice ( $n = 3$ -6/group). Horizontal lines show mean. Each symbol represents an individual mouse. Data are pooled from two experiments with similar results.

**Fig. S5.** Representative FACS plots showing gating strategy used to characterized cytokine production by CD4<sup>+</sup> and CD8<sup>+</sup> T cells. The representative sample is from LI.

**Fig. S6.** MLN and lamina propria mononuclear cells from WT, *PTPN22*<sup>-/-</sup>, *IL-10*<sup>-/-</sup>, and *PTPN22*<sup>-/-</sup>*IL-10*<sup>-/-</sup> mice treated with DSS for 8 days were processed, stained, fixed and permeabilized to assess IFN- $\gamma$  and TNF by CD8<sup>+</sup> T cells (a) Representative FACS plots display frequency of IFN- $\gamma$ TNF<sup>+</sup>, IFN- $\gamma$ <sup>+</sup>TNF<sup>+</sup> and IFN- $\gamma$ <sup>+</sup>TNF<sup>-</sup> CD8 T cells from the LI. A representative mouse from each strain is shown. (b-c) Graphs display frequency in MLN (b) and LI (c) from multiple mice ( $n = 3-6$ /group). Horizontal lines show mean. Each symbol represents an individual mouse. Data are pooled from two experiments with similar results.

**Fig. S7.** Representative FACS plots showing gating strategy used to characterized innate immune cells. The sub-population analysed are lymphoid DCs (CD11b<sup>-</sup>CD11c<sup>+</sup>),

myeloid DCs (CD11b<sup>+</sup>CD11c<sup>+</sup>) and other myeloid cells (CD11b<sup>+</sup>CD11c<sup>-</sup>). Following gating on CD11b<sup>+</sup>CD11c<sup>-</sup> we characterized neutrophils (F4/80<sup>-</sup>LY6G<sup>+</sup>) and macrophages (F4/80<sup>+</sup>LY6G<sup>-</sup>). Further gating on F4/80<sup>+</sup> cells enabled the characterization of monocytes and macrophages and eosinophils. The representative sample is from LI of a *PTPN22*<sup>-/-</sup>*IL-10*<sup>-/-</sup> mouse.

**Fig. S8.** Innate immune cell distribution. MLN and LI of DSS-treated mice (*WT*, *PTPN22*<sup>-/-</sup>, *IL-10*<sup>-/-</sup> and *PTPN22*<sup>-/-</sup>*IL-10*<sup>-/-</sup>) were processed and stained to assess the composition of innate immune cells during acute experimental colitis. (a) Representative graphs display frequency of innate cells in MLN. (b) Frequency of innate cells in LI is displayed. Each symbol represents an individual mouse.

**Table S1.** List of the antibodies and fluorophore conjugates used, including the dye, commercial source, clone and catalog number.